metals

MDPI

Article

Pattern Formation by Spinodal Decomposition in Ternary Lead-Free Sn-Ag-Cu Solder Alloy

Jia Sun [1], Huaxin Liang [1], Shaofu Sun [2], Juntao Hu [1], Chunyu Teng [3], Lingyan Zhao [1,*] and Hailong Bai [1,*]

[1] R&D Center of Yunnan Tin Group (Holding) Co., Ltd., Kunming 650106, China
[2] Tin Products Manufacturing Co., Ltd. of Yunnan Tin Group (Holding) Co., Ltd., Kunming 650501, China
[3] AVIC China Aero-Poly Technology Establishment, Beijing 100028, China
* Correspondence: zhaoly_ytc@163.com (L.Z.); baihl_ytc@163.com (H.B.)

Abstract: In comparison to Pb-based solders which have a toxic effect, the tin-silver-copper (SAC) family of alloys have relatively strong reliability and are widely used in the electronics industry. Phase separation and coarsening phenomenon on the surface of 96.5 wt. % Sn-3.0 wt. % Ag-0.5 wt. % Cu (SAC305) solder products exhibit special microstructural features and offer opportunities for the microstructure control of microelectronic interconnects. However, the formation mechanism of such morphological patterns is still unknown. Here, we applied a combination of experimental and phase field methods to study how such patterns form. It was observed that the pattern was Sn-rich and exhibited the characteristic morphology of spinodal decomposition. Contrary to earlier findings that only binary systems like Sn-Pb and Sn-Bi experienced such phenomena, spinodal decomposition was firstly observed in ternary solder system Sn-Ag-Cu. Morphology of Sn-rich patterns depended on whether the spinodal decomposition reacted completely. SAC305 solder alloy was easily decomposed by Sn component after being heated to roughly 260 °C. The above conclusions could offer theoretical support for quantitatively controlling the microstructure of solder alloys and would enhance the quality of related products.

Keywords: Pb-free solder; phase field method; spinodal decomposition; SAC alloy

Citation: Sun, J.; Liang, H.; Sun, S.; Hu, J.; Teng, C.; Zhao, L.; Bai, H. Pattern Formation by Spinodal Decomposition in Ternary Lead-Free Sn-Ag-Cu Solder Alloy. *Metals* **2022**, *12*, 1640. https://doi.org/10.3390/met12101640

Academic Editor: Jan Vrestal

Received: 27 August 2022
Accepted: 22 September 2022
Published: 29 September 2022

Publisher's Note: MDPI stays neutral with regard to jurisdictional claims in published maps and institutional affiliations.

Copyright: © 2022 by the authors. Licensee MDPI, Basel, Switzerland. This article is an open access article distributed under the terms and conditions of the Creative Commons Attribution (CC BY) license (https://creativecommons.org/licenses/by/4.0/).

1. Introduction

Solders represent highly useful and versatile materials. They provide a broad range of technical applications such as soldering in micro electro-mechanical systems (MEMS) [1]. Sn-Ag-Cu solder system is one of the most promising and mainstream lead-free alloys for its relatively low melting point, low cost, excellent mechanical properties and other merits [2,3]. It is known that the reliability of packages depends strongly on the microstructure of solder interconnects. However, there are still some issues preventing further application of SAC305 alloys, one of which is the matt-like Sn-rich hump structures distributed on the surface of BGA (balls grid array package) solder balls and SAC305 powder, which can greatly decrease the reliability of the solder joint. Many factors may account for such damage. Microstructural changes such as phase decomposition and coarsening may affect the overall properties of the joints [4]. Firstly, phases separated by decomposition and coarsening can cause solder balls to skew during service, thus resulting in short circuit between solder bumps in BGA [5]; furthermore, the inherent tendency of microstructure coarsening and phase segregation in solder alloys under thermal loading can easily lead to the inhomogeneous mechanical and thermal response behaviors, which can promote crack initiation and expansion near the interface between the major phases, and this has brought about serious reliability concern for the above applications [6]. In particular, the coarsening of phases generates domains which are susceptible to mechanical failure. Experimental observations show that voids, crack initiation and crack propagation are prevalent along phase boundaries. These phenomena lead to variations in the deformation behavior of the

SAC305 solder during service and raise concerns about their predictability and long-term reliability. Many attempts have been made to shed light on the formation of the Sn-rich phase microstructure in binary alloy systems by combined phase field methods and experimental tools. Anders [4] et al. presented numerical simulations of phase decomposition and coarsening controlled by diffusion for eutectic binary solders Sn-Pb and Ag-Cu, a three-dimensional phase separation event within a solder balls geometry corroborates the quality of the model well. Tawakoni [7] et al. introduced a quantitative phase-field approach to study the phase-coarsening phenomena in Pb-Sn solder alloys, which method can quantify the experimental and simulation data without putting into difficulties corresponding to the stochastic nature of phenomenon. Davidoff [8] et al. investigated spinodal decomposed patterns in rapidly quenched Co-Cu melts. Experimental results consisted with predictions of computational modeling using a model of fast spinodal decomposition in these investigations. It is commonly recognized that the combination of experimental research and numerical simulation to reproduce the process of microstructural evolution is conducive to comprehensively understand the law of the evolution and its influencing factors [9]. To explore deeply the formation process of the pattern formed by spinodal decomposition in binary solder alloy system, experimental approaches and phase field simulations were developed and showed better characteristics for phase separation and coarsen, but the entire formation mechanism of the Sn-rich phase pattern in solder of ternary Sn-Ag-Cu system has not been studied theoretically by microstructure simulation combined with experiments. In the present study, we focus on the spinodal decomposition process in ternary Sn-Ag-Cu system since it plays an important role on microstructure and properties of the solder joints. For this purpose, a phase field model based on the Cahn-Hilliard equation is introduced to simulate the coarsening process in tin lead-free solders since phase field modeling has evolved into a powerful tool for computational materials science over the past years. Formation mechanism of spinodal decomposed structure is the basis of controlling the proportion of surface microstructure on solder ball in industrial production.

2. Materials and Methods

2.1. Experiments

Figure 1 is the schematic diagram of the solder joint and the scanning electron microscope (SEM) photo of solder balls applied in BGA of microelectronic packaging. As can be seen in Figure 1, the surface structure of solder balls has a great influence on the soldering performance of the solder ball since they connect with the Cu pad directly. Samples of BGA solder balls in this report were produced by the "piezoelectric vibration method" and provided by Yunnan Tin Material Co., LTD. Specimens with a nominal composition 96.6 Sn 2.88 Ag 0.468 Cu (wt. %) were alloyed by arc melting under a nitrogen atmosphere. At the same time, oxygen was added since only nitrogen protection can easily lead to adhesion of powder. The production process of solder alloy products was as follows: the shooting balls temperature was 260 °C, cooling temperature was 45–50 °C for the first section and the second to fourth section was −20 °C. The length of each section was 1.5 m.

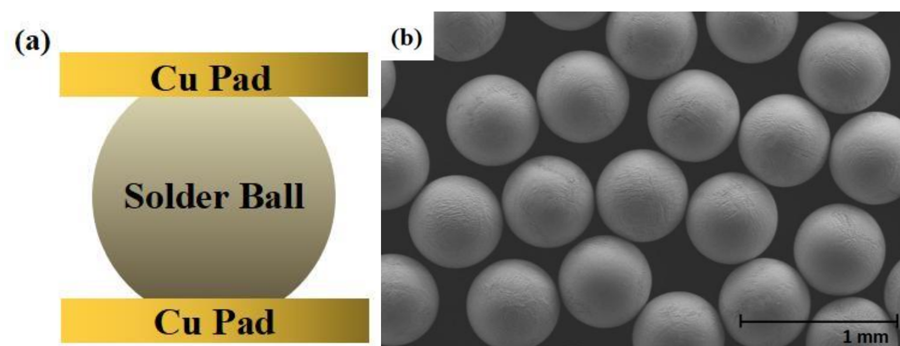

Figure 1. (**a**) Schematic diagram of the solder joint and (**b**) SEM photo of solder balls.

Samples of solder powder were produced by the "pinning disc centrifugal atomization method" and also provided by Yunnan Tin Material Co., LTD. The diameter of rotating disc was about 70 mm, the rotating speed of the motor was 35,000 r/min under the condition of 100 kg/h. Solder powder was prepared by melting the pure Sn, Ag and Cu according to a certain composition in an intermediate frequency furnace to produce tin base alloy. Then the alloy was heated to 240~350 °C to melt. After completely melted, the liquid alloy flowed to high-speed disc through the guide pipe to form powder by atomization. The atomizing atmosphere was mainly inert gas nitrogen. To ensure the homogeneity of the alloy, the samples were carefully shaken and mixed during melting. The purpose of mixing was to obtain powder balls with a fine microstructure, which is characteristic for a solder interconnection used in microelectronics.

Samples were examined by Hitachi SU8010 (Hitachi, Japan) using and a cross beam workstation equipped with an energy-dispersive IXRF 550i X-ray spectrometry system. The K-alpha X-ray photoelectron spectrometer made by Thermofisher company (Waltham, MA, USA) was applied to examine the specimens.

2.2. Phase Field Model

Phase coarsening in tin lead-free solders frequently happens because of the spinodal decomposition. To verify the Sn-rich phase patterns and their development in spinodal decomposition, we provide a phase field computational modeling of phase separation. This equation is currently known as the Cahn-Hilliard [10,11] equation. Later, this equation was used by Dreyer and Müller [12–14] to study the phase coarsening transformation.

According to Cahn-Hilliard model mentioned above, the total free energy F of an inhomogeneous mixture at the constant temperature T could be approximated by the following energy functional:

$$F = \int \left\{ f(c,t) + \frac{1}{2}\kappa(\nabla c)^2 \right\} dV \quad (1)$$

κ is the gradient energy coefficient and $f(c,t)$ is the chemical/bulk energy of homogeneous material of composition represented by:

$$f(c) = Ac^2(1-c)^2 \quad (2)$$

which is a simple phenomenological double-well potential. A is a positive constant and controls the magnitude of the energy barrier between two equilibrium phases. The form of the system, based on the diffusion equation and supplemented by appropriate boundary conditions, reads:

$$\frac{\partial c}{\partial t} = \nabla^2 M \frac{\partial F}{\partial c} + \xi_i \quad (3)$$

where M is the diffusion mobility. The 2D computational supercell was discretized into a system of 256 $\times$ 256 grids with $dx = dy = 1.0$. ξ_i is the thermal noise and supposed to be a precursor for spinodal decomposition phase transformations. Periodic boundary conditions were assumed along the x- and y-directions, and all of the parameters used in the simulation were non-dimensional. All of the parameters used in the simulation are nondimensional. The time increment Δt per time step was set as $\Delta t = 0.01$ in Euler time integration. The simulation was carried out up to 10,000 Δt for the system would reach equilibrium at this time. Fortran language was applied to code the phase field model.

3. Results and Discussion

The methods of both experiments and phase field simulation were combined to investigate the formation process of Sn-rich phase microstructure on SAC305 balls and powder products. Results show that experiments consist well with the simulation as discussed below.

3.1. Microstructural Characteristics by Experimental Methods

Morphologies or patterns are shaped by the complex dynamical evolution of the solid-liquid interface and are both intricate and varied. Figure 2 shows the microstructure of a BGA solder ball. It can be seen from Figure 2a,b that many continuous humps distributed on a solder ball surface and there were both smooth areas (zone A) and rough areas (zone B). The micrographs clearly illustrate the diffusion induced phase separation in the considered Sn-Ag-Cu system. Details of the BGA solder ball are shown at higher magnification in Figure 2c,d imaged by SEM. As a rule, worm-like structure which is typically observed in spinodal decomposition was found on the solder ball surface. Generally, non-bright humps area had two kinds of shape form: firstly, rod humps regularly precipitated with long sides connected with each other as shown in the dashed line box in Figure 2c; secondly, nearly round shape distributed randomly as shown in the dotted circle in Figure 2b. These matt-like humps distributed discretely were nearly oval in cross-section with a diameter of about 1~10 μm. Moreover, most of worm-like humps on a solder ball surface were rod-like and with length of about 20 μm and short edge 5 μm; the periodicity as a mean distance between two neighboring structures ranged from 2 to 5 μm. Additionally, many inter-metallic compound (hereinafter referred to as IMC) Ag_3Sn particles dispersed on the solder ball surface. They precipitated along humps like "necklace" as the dashed curve in Figure 2d indicates. The regular distribution of Ag_3Sn indicates that the approximate spinodal decomposed patterns form firstly and then the Ag_3Sn precipitates afterwards. It was reported that cracks on the surfaces of solder powder balls would initiate more easily than that in solder balls since there were more trenches on the surface of the latter [6]. Otherwise, the matt-like morphology on the ball surface can cause blurred vision during BGA ball mounting. Therefore, it is quite necessary to study the formation mechanism of such morphology so as to control the surface structure of BGA balls.

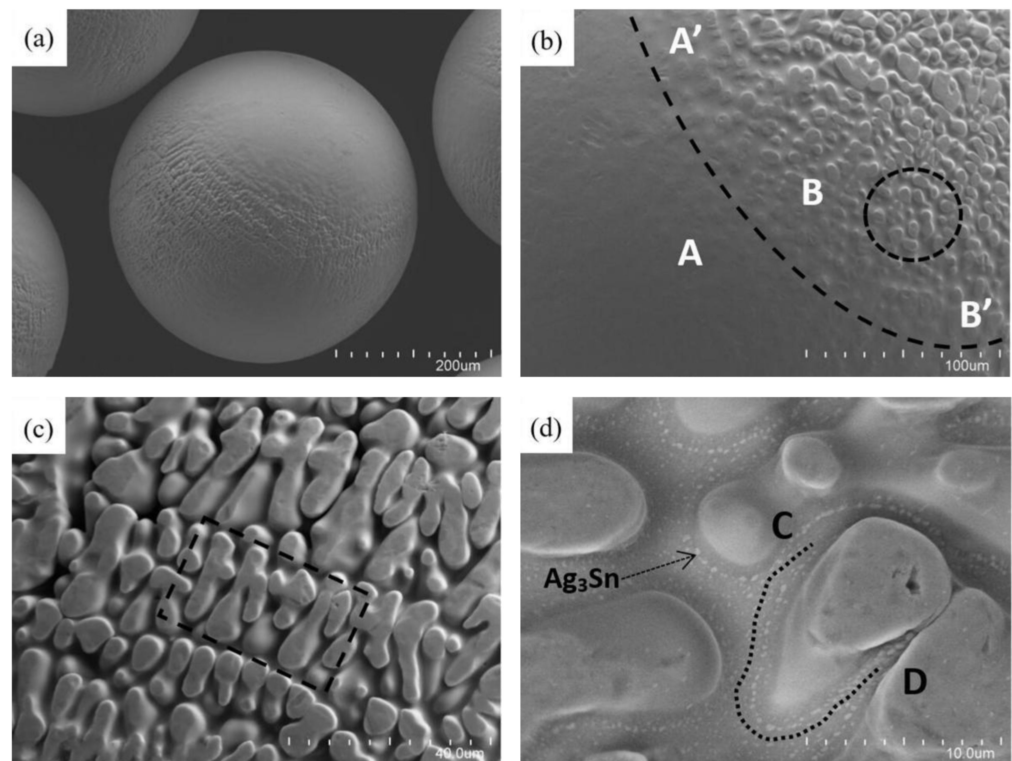

Figure 2. (**a**) The morphology of surface of BGA solder balls; (**b**) zoomed view of glossy area (A) and matt-like area (B) distinguished by dashed line A'B'; (**c**) the nearly rod-like humps that arranged periodically; (**d**) the nearly-oval humps and Ag_3Sn particles that precipitated around a hump marked by dashed curve CD.

EDS experiments were carried out in order to study the composition of humps, as Figure 3 shows. The EDS scanning experiment results show that the composition of humps was pure Sn (100 wt. %), as shown in Figure 3b. The matrix of the solder ball contained three elements Sn, Ag and Cu, and the content (96.6 Sn 2.88 Ag 0.468 Cu) was roughly the same as products of solder balls, as shown in Figure 3c. As can be seen, two phases of different composition emerged, where the hump areas were the Sn-rich phase and the other was the matrix area of solder ball. The Sn content on the solder ball surface was 93.44 wt. %. The EDS results indicated that it was the component Sn diffused out of the solder ball surface to form the Sn-rich phase up to the "matt-like" morphology. In conclusion, the Sn-rich phase distributed unevenly in the SAC305 alloy matrix of the solder interconnect during thermal aging, which formed the morphology of coexistence of smooth and rough areas as Figure 2b presents.

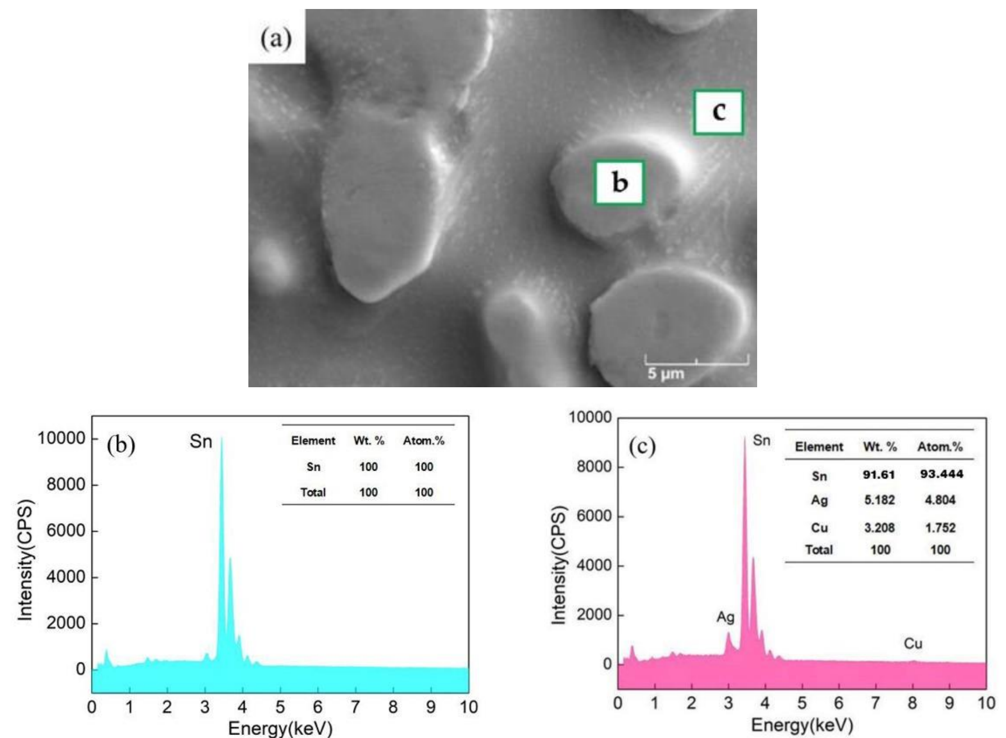

Figure 3. (**a**) Zoomed view of humps (**b**) and matrix (**c**); EDS experiments of (**b**) humps and (**c**) matrix.

The elemental SEM-EDS mapping was performed in Figure 4 to further study the composition distribution of SAC305 solder ball. As seen, Sn contrast (in green) was higher in the Sn-rich phase than that in the alloy matrix, while its intensity decreased in the Ag_3Sn IMC regions. The distribution of different shades of red, yellow and green indicated that the originally mix of Sn, Ag and Cu was superseded by islands of high Sn concentration. These form as a result of a diffusion driven separation of both phases known as coarsening [15]. Ag (in yellow) widely distributed on the solder matrix with obvious edges compared with Sn and Cu, which can be deduced to be the reason that many Ag_3Sn formed on the solder ball surface. These results also indicated that Ag was consumed in the formation of Ag_3Sn IMC. The presence of Cu (in red) was not obvious due to its relatively low content. Therefore, it is confirmed that the formation of the Sn-rich phase was the diffusion of Sn from low concentration to high concentration. In other words, Sn separated from the matrix to form Sn-rich phase with a certain composition higher than that of the solder ball. The alloy spontaneously disintegrates into Sn-rich poor phase and matrix [16]. Moreover, there was no obvious phase interface between Sn-rich phase and the SAC305 matrix. To sum up, this micromorphological change was a result of a diffusion process of the component Sn, also known as spinodal decomposition, followed by coarsening through phase separation. In other words, spinodal decomposition was realized through spontaneous growth of

fluctuations of Sn composition. Consequently, this process of Sn phase separation led to worm-like stochastically orientated patterns. Heat treatments during production yielded a fluctuation of component distribution, formed during heating, with evidence supporting its formation to be via spinodal decomposition [17]. Such types of phase separation can be accelerated considerably if the homologous temperatures are high [18]. For example, it was reported by Kaban et al. [19] that the surface tension of the investigated Sn-Ag-Cu alloys strongly depends on Sn concentration. The surface tension decreases rapidly with small additions of Sn and varies weakly with composition in the Sn-rich region. Since the Sn concentration was high in SAC305 alloy, when slight Sn diffused out of matrix to take shape into humps (Sn content was slightly higher in humps (100 wt. %) than that in the matrix (96.5 wt. %)), the surface tension decreased fleetly to form humps with different shapes, thus promoting the formation of Sn-rich patterns. As the spinodal decomposition processed, surface tension inside these Sn-rich humps was quite small and could not stimulate new humps to take shape. Consequently, no more structure changes took place after the spinodal decomposition. Rather, changes in microstructure due to spinodal decomposition were also observed in Sn-Pb, Co-Cu [8] and Ag-Cu [20] alloys, most of which were binary systems. Nevertheless, it is the first time that spinodal decomposition of the single component Sn in ternary Sn-Ag-Cu solder alloy was discovered, which is unprecedented that spinodal decomposition took place in solder alloys were all in binary systems.

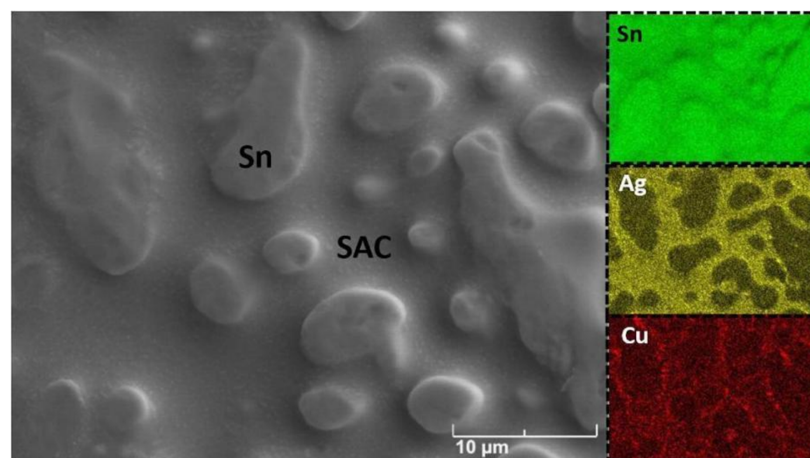

Figure 4. The SEM-EDS map scanning analysis on a local part of BGA solder ball which shows the map scanning results of Sn, Ag and Cu elements.

Spherical solder powder is a new type of electronic solder material. It is widely applied as solder paste for electronic surface mount technology (SMT). The microstructure of the SAC305 solder powder also exhibited spinodal patterns when analyzed by SEM as Figure 5 shows. The Sn-rich "worm" structures were about 2.5 µm in diameter. Additionally, the surface characteristics of SAC305 solder powder were basically the same as that of the solder ball as Figure 2 presents. However, there were still some microstructure differences between the Sn-rich phase patterns on two products. On one hand, Sn-rich phase on solder powder ball surface closely connected each other with almost no trenches between them; on the other hand, Ag_3Sn precipitated more uniformly on the surface of solder powder than that on solder balls. It can be seen that many Ag_3Sn particles also distributed on the surface of Sn-rich phase, which was quite different from the phenomena that Ag_3Sn was mainly distributed in trenches between Sn-rich phase in solder balls. Such a discrepancy indicated that the precipitation sequence of Sn-rich phase and Ag_3Sn particles was not clear during the production process of solder powder. The starting composition fluctuations would undergo phase separation via spinodal decomposition, in which domains within the humps possessed local chemical enrichment of certain element Sn. A conclusion can be drawn by combining the results of BGA solder balls and powder that spinodal decomposition of Sn can happen very easily on spheroidal and ternary SAC305 solder alloy, which is

supposedly owing to the reason that the interstitial diffusion in Sn can enhance the flux of thermal migration [21]. Moreover, the oxygen in the protective gas during production of solder products also promoted the formation of Sn-rich phase since the driving force for the spinodal decomposition increased as the oxygen content increased [22]. In experimental processes such as hot rolling, spinodal decomposition occurs at high temperatures. One of the most prominent features of solder alloys is that its microstructure is more prone to show phase coarsening and segregation characteristics, bringing about an increasing concern on reliability of SAC305 solder interconnects. In other words, the spinodal decomposed structure on surface of solder powder balls will affect the coating performance with the solder paste. In any case overall the material properties of the solder change over time which, eventually, has a detrimental effect on its joining capability.

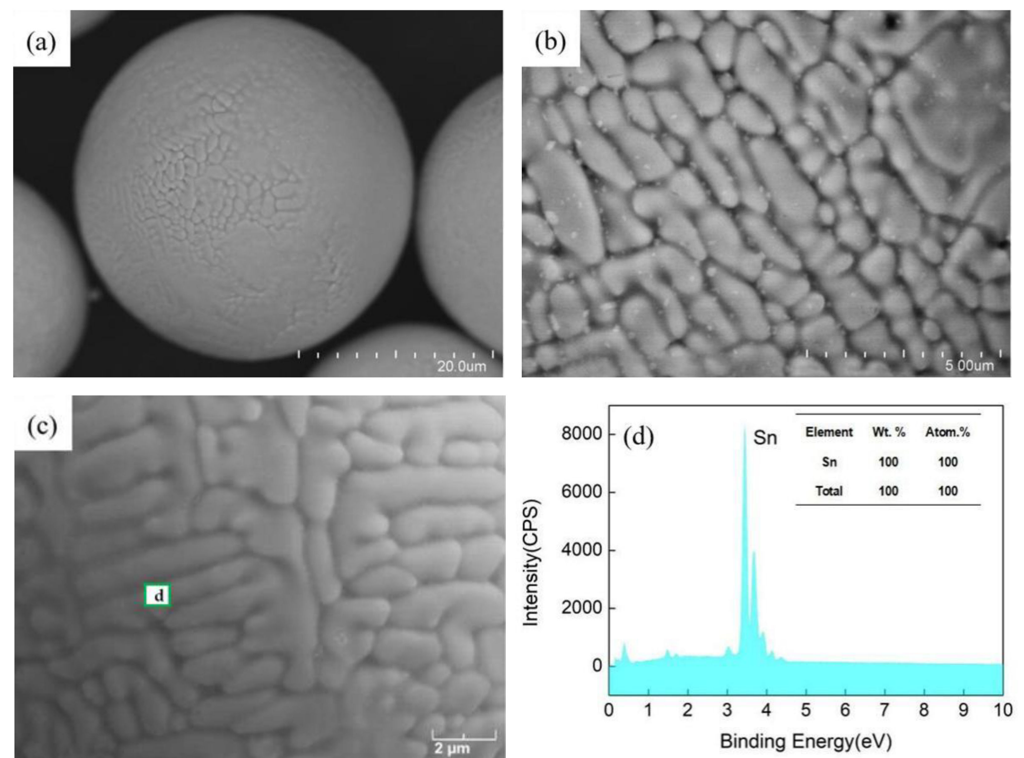

Figure 5. The SEM microstructure of the solder powder (**a**–**c**) and (**d**) the relative EDS results of Sn-rich phase as square d points in (**c**) on the solder powder ball surface.

The XPS patterns of Sn 3d peaks for surfaces of a SAC305 solder ball and powder samples are shown in Figure 6. Both specimens showed similar features: the single peak curves of the surface were composed of three curves: Sn, Sn^{2+} and Sn^{4+} curves; there were two kinds of chemical states of Sn: Sn oxides and metallic Sn; the peak position of metallic Sn was located at about 484.8 eV, while the peaks standing for tin oxides Sn^{2+} and Sn^{4+} were showing at 486~487 eV. However, it can be seen that the peak of Sn^{4+} in the ball was stronger than that in powder; on the contrary, another Sn^{2+} peak was stronger in powder than that in the BGA ball. It turned out that there were various degrees of oxidative effect in both SAC305 solder balls and powder.

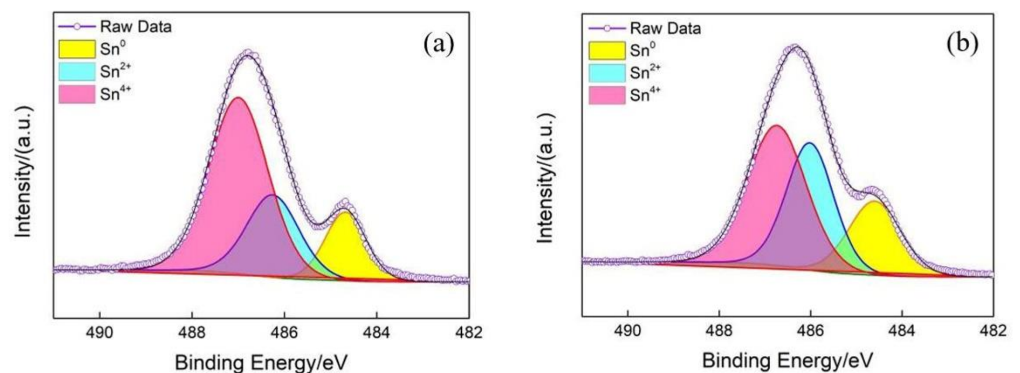

Figure 6. The XPS patterns of Sn 3d peaks for SAC305 solder (**a**) ball and (**b**) powder.

3.2. Microstructural Evolution by Phase Field Simulation

To the best of the authors' knowledge, patterns of spinodal decomposition in high-temperature metallic liquids (particularly, in Sn-Ag-Cu ternary alloy) have not previously been observed and described in the available literature. Spinodal decomposition will not be observed in experiments because the transition is very fast. Therefore, results of phase field simulations were applied and also confirmed the above discovery about spinodal decomposition in the Sn-Ag-Cu ternary system to detect deeply the reaction process [23]. Time evolution of the 2D microstructure version of phase separation was summarized in Figure 7a–e. As can be seen at t = 20 time in Figure 7a, the microstructure was relatively fine and contained a large number of precipitates, leading to a small distance between phases which might cause an increase in the alloy strength because a higher opposition to the dislocation movement exists [24]. There were more rod-like Sn-rich phases at the earlier stage of spinodal decomposition, which was presumed to be the reason that the composition at this moment had not fluctuated completely yet. As the aging time progressed, coarsening of the second phase through migration of the phase boundaries, dissolution, merging, and breakup could be easily inferred from the Figure 7b. The large size Sn-rich phase particles grew up at the expense of the small size ones, thus forming the stochastic worm-like morphology as black dashed circle in Figure 7d shows. The growth of the Sn-rich phase mainly occurred with Ostwald ripening process in which the small precipitates dissolved and absorbed by the larger ones, and as a result the number of precipitates became smaller with time. However, the number of the long-rod-shaped Sn-rich phase significantly reduced and rounder Sn-rich phase formed discretely when the reaction was almost complete at t = 100. Conclusively, it was the incomplete spinodal decomposition that caused the formation of continuous rod-like Sn-rich phase as the black dashed circle in Figure 7d shows; the discrete round Sn-rich phase region proved that the spinodal decomposition phase separation had reacted completely as the white dashed circle in Figure 7e presents. It is worth indicating that the simulation results presented in Figure 7 exhibit some discrepancies from the experimental observation, in which the rod-like Sn-rich phase particles distribute randomly rather than precipitate regularly with long sides connecting closely as shown in Figure 2c. This is because the experimental observations are usually influenced by more factors, such as the formation of IMC, anisotropies of surface energy and grain boundaries [9]. Despite these limitations, the simulated characteristics of the microstructure were largely consistent with the experimental observations. In conclusion, the formation mechanism of the Sn-rich phase pattern microstructure on the surface of SAC305 alloy is the spinodal decomposition of Sn according to results of both experimental investigation and phase field simulation.

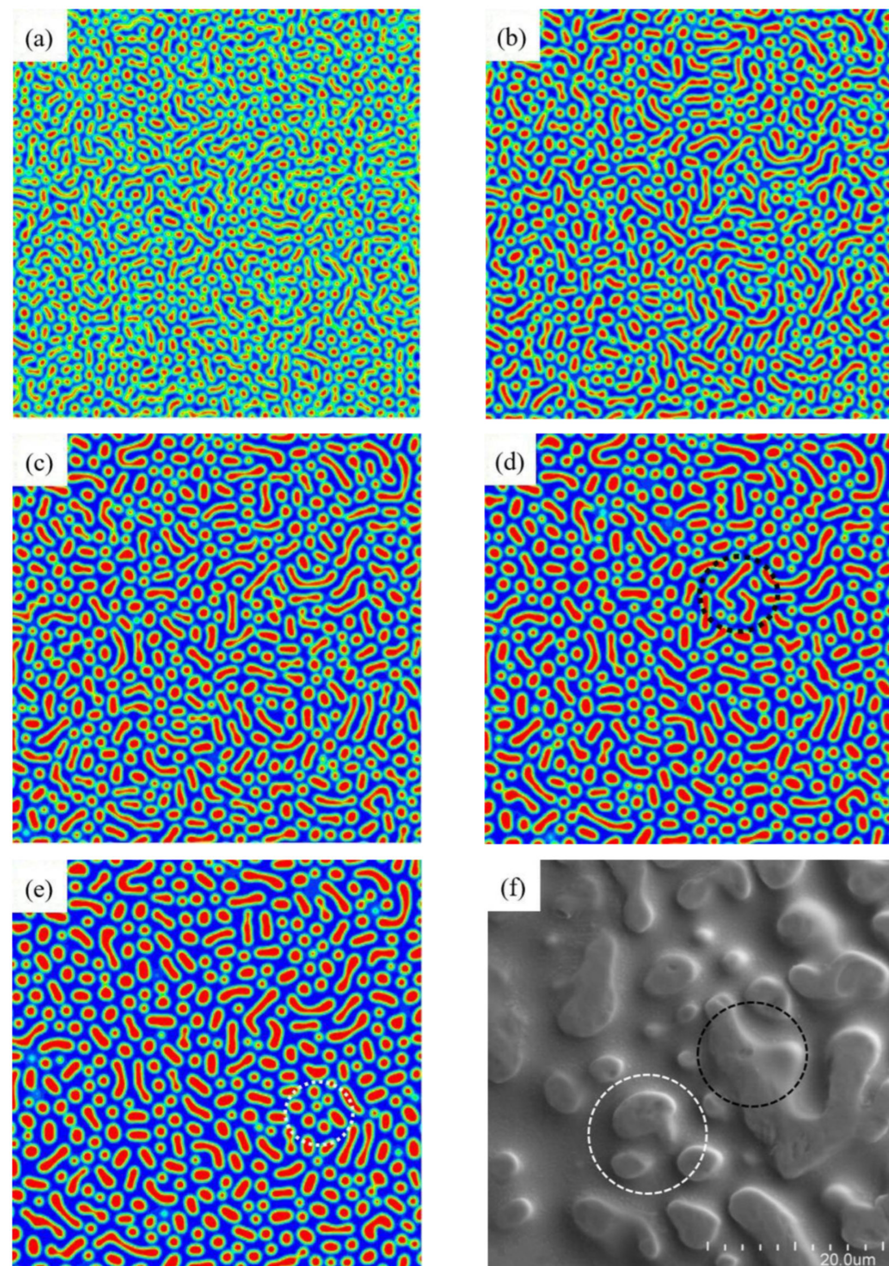

Figure 7. Time evolution of the microstructure due to spinodal decomposition by the phase field simulations: (**a**) $t = 20$; (**b**) $t = 40$; (**c**) $t = 60$; (**d**) $t = 80$; (**e**) $t = 100$; (**f**) a SEM image showing the pattern and morphology of Sn-rich phase patterns that consistent well with simulation results.

Figure 8 shows the volume fraction of spinodal decomposition patterns and the evolution of total free energy according to reaction time in the phase field simulation results that show the kinetics of spinodal decomposition. The plot in Figure 8a shows an increase in volume fraction with time up to about $t = 30$. Then, the growth kinetic rate was decelerated, and subsequently the volume fraction remained almost constant. This fact indicated that the phase decomposition finished, and the coarsening of the decomposed phases began at about $t = 90$. This stage was characterized by the growth of the Sn-rich phase at the expense of the smaller ones, as can be seen in Figure 8b. It can be deduced that higher total free energy provided stronger fluctuation in concentration at early stage, which promoted the nucleation and subsequent growth of large and continuous rod-like Sn-rich phase. As phase separation proceeded, the large Sn-rich phase swallowed up small ones so as to form stable microstructure, which was consistent with the theory that large particles grew at

the expense of smaller ones in diffusion-controlled coarsening [25]. The decomposition was determined solely by diffusion of Sn element since there was no thermodynamic barrier to the reaction inside of the spinodal region [7]. After this time t = 120, the Sn-rich phase formed morphologically stable spherical precipitates as the interfacial energy of the precipitates reduced via coarsening, as expected from the Cahn-Hilliard model for spinodal decomposition [11]. In conclusion, it is necessary to strictly control the aging time since this processing parameter does have a prominent effect on microstructure of solder alloys. Additionally, it is reported that the presence of the phase decomposition was responsible for the increase in hardness, which improved the overall property of the alloys [26].

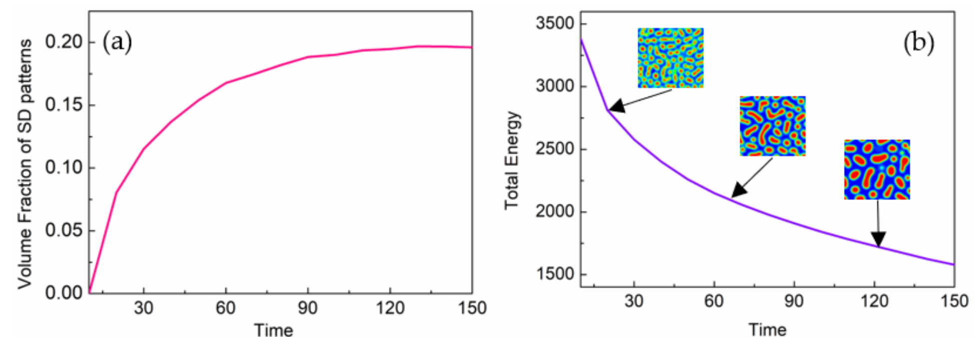

Figure 8. (**a**) Volume fraction of spinodal decomposition patterns; (**b**) time variation of the discrete free energy with the insets showing the microstructures at times indicated by the arrows.

The thermal stress and temperature gradient at the interface between the separated phases and solder microstructure are high, which can promote the crack initiation and expansion and even cause deterioration of the reliability of solder joints [27]. Thus, it is meaningful to characterize the microstructural evolution of such phase separation and coarsening of solders in interconnects. Nevertheless, the current model had some limitations. The phase field model only explained the corresponding spinodal decomposition phenomenon but did not correspond to the alloy composition of SAC305, which was included in our on-going investigation work. Furthermore, how to quantitatively control the area ratio of the Sn-rich phase and glossy part on the surface of solder balls was another meaningful task due to its effects on reliability of solder balls and powder, as mentioned in the introduction part of this article.

4. Conclusions

The spinodal decomposition of SAC305 solder balls and powder were investigated by experimental methods combined with Cahn-Hilliard phase field model. Spinodal decomposition in ternary solder alloy was firstly discovered. Component Sn in ternary Sn-Ag-Cu system diffused out from the matrix to take shape as the Sn-rich phase, thus forming the mist-like pattern that consisted of the Sn-rich phase. Periodical continuous rod-like Sn-rich phases formed if the spinodal decomposition processed incompletely; on the contrary, fully reacted spinodal decomposition resulted in discrete oval Sn-rich hump morphology. Both SAC305 solder balls and powder surfaces showed oxidative effect. IMC Ag_3Sn precipitated after spinodal decomposition of the Sn-rich phase on BGA solder balls. These results shed light on the formation reason of phase separation patterns on SAC305 solder products, which provided strong theoretical basis for controlling the process technology which determined the microstructure in the production of BGA solder ball and powder products.

Author Contributions: Conceptualization, L.Z. and J.S.; methodology, J.S.; software, J.S. and J.H.; validation, J.S., H.L. and J.H.; formal analysis, L.Z. and S.S.; investigation, L.Z. and J.S.; resources, S.S.; data curation, J.S. and J.H.; writing-original draft preparation, J.S.; writing-review and editing, J.S. and C.T.; visualization, J.S.; supervision, H.B.; project administration, H.B. and L.Z.; funding acquisition, H.B. and L.Z. All authors have read and agreed to the published version of the manuscript.

Funding: This research was funded by Applied Basic Research Foundation of Yunnan Province, grant number 202101BC070001-010 and Chuncheng Project III.

Data Availability Statement: The data presented in this study are available upon request from the corresponding author. The data are not publicly available due to the fact of technical or time limitations.

Acknowledgments: The authors are grateful to Shaofu Sun, Lingyan Zhao and Hailong Bai for their contribution to the discussion.

Conflicts of Interest: The authors declare no conflict of interest.

References

1. Illés, B.; Krammer, O.; Géczy, A. *Reflow Soldering: Apparatus and Heat Transfer Processes*; Elsevier: Amsterdam, The Netherlands, 2020.
2. Dušek, K.; Bušek, D.; Veselý, P.; Pražanová, A.; Plăcek, M.; Del, R.J. Understanding the Effect of Reflow Profile on the Metallurgical Properties of Tin-Bismuth Solders. *Metals* **2022**, *12*, 121. [CrossRef]
3. Kang, Y.B.; Choi, J.J.; Kim, D.G.; Shim, H.W. The Effect of Bi and Zn Additives on Sn-Ag-Cu Lead-free Solder Alloys for Ag Reduction. *Metals* **2022**, *12*, 1245. [CrossRef]
4. Anders, D.; Hesch, C.; Weinberg, K. Computational Modeling of Phase Separation and Coarsening in Solder Alloys. *Nt. J. Solids. Struct.* **2012**, *49*, 1557–1572. [CrossRef]
5. Depiver, A.; Mallik, S.; Amalu, E.H. Thermal Fatigue Life of Ball Grid Array (BGA) Solder Joints Made from Different Alloy Compositions. *Eng. Fail. Anal.* **2021**, *125*, 105447. [CrossRef]
6. Liang, S.B.; Ke, C.B.; Huang, J.Q.; Zhou, M.B.; Zhang, X.P. Phase field simulation of microstructural evolution and thermomigration induced phase segregation in Cu/Sn58Bi/Cu interconnects under isothermal aging and temperature gradient. *Microelectron. Reliab.* **2019**, *92*, 1–11. [CrossRef]
7. Tavakoli, M.M.; Tavakoli, R.; Davami, P.; Aashuri, H. A Quantitative Approach to Study Solid State Phase Coarsening in Solder Alloys Using Combined Phase-Field Modeling and Experimental Observation. *J. Comput. Electron.* **2014**, *13*, 425–431. [CrossRef]
8. Davidoff, E.; Galenko, P.K.; Herlach, D.M.; Kolbe, M.; Wanderka, N. Spinodally Decomposed Patterns in Rapidly Quenched Co-Cu Melts. *Acta. Mater.* **2013**, *61*, 1078–1092. [CrossRef]
9. Ke, C.B.; Zhou, M.B.; Zhang, X.P. Phase Field Simulation on Microstructure and Growth Kinetics of Cu_6Sn_5 Intermetallic Compound during Early Interfacial Reaction in Sn/Cu Soldering System. *Acta. Metall. Sin.* **2014**, *50*, 294–304.
10. Cahn, J.W.; Hilliard, J.E. Free Energy of A Nonuniform System I: Interfacial Free Energy. *J. Chem. Phys.* **1957**, *28*, 258–267. [CrossRef]
11. Cahn, J.W. Spinodal Decomposition. *Trans. Metall. Soc. AIME* **1968**, *242*, 166–180.
12. Dreyer, W.; Müller, W.H. A Study of the Coarsening in Tin/Lead Solders. *J. Mater. Sci.* **2000**, *37*, 3841–3871. [CrossRef]
13. Dreyer, W.; Wagner, B. Sharp-Interface Model for Eutectic Alloys Part I: Concentration Dependent Surface Tension. *Interface. Free. Bound.* **2005**, *5*, 199–227. [CrossRef]
14. Böhme, T.; Dreyer, W.; Müller, W.H. Determination of Stiffness and Higher Gradient Coefficients by Means of the Embedded-atom Method. *Contin. Mech. Thermodyn.* **2007**, *18*, 411–441. [CrossRef]
15. Dreyer, W.; Müller, W.H. Modeling Diffusional Coarsening in Eutectic Tin/Lead Solders: A Quantitative Approach. *Int. J. Solids. Struct.* **2001**, *38*, 1433–1458. [CrossRef]
16. Jiang, B.H.; Chang, M.H.; Wei, Q.; Xu, Z.Y. Thermodynamical Criterion of Spinodal Decomposition in Ternary System. *Acta. Metall. Sin.* **1990**, *26*, B303–B309. [CrossRef]
17. Collins, D.M.; Souza, N.D.; Panwisawas, C.; Papadaki, C.; West, G.D.; Kontis, A.K.P. Spinodal Decomposition Versus Classical γ' Nucleation in A Nickel-base Superalloy Powder: An In-situ Neutron Diffraction and Atomic-scale Analysis. *Acta. Materia.* **2020**, *200*, 959–970. [CrossRef]
18. Müller, W.H.; Böhme, T. Coarsening Processes in the Lead-free Solder Alloy AgCu: Theoretical and Experimental Investigations. In Proceedings of the 2005 IEEE 6th Electronic Components and Technology Conference, Shenzhen, China, 30 August–2 September 2005; pp. 613–617.
19. Kaban, I.; Gruner, S.; Hoyer, W. Surface Tension and Density in Liquid Ag-Cu-Sn Alloys. *J. Non Cryst. Solids.* **2007**, *353*, 3717–3721. [CrossRef]
20. Tanaka, Y.; Udoh, K.-I.; Hisatsun, K.; Yasuda, K. Spinodal Ordering in the Equiatomic AuCu Alloy. *Philos. Mag.* **1994**, *69*, 925–938. [CrossRef]
21. Chen, C.; Hsiao, H.Y.; Chang, Y.W.; Ouyang, F.; Tu, K.N. Thermomigration in Solder Joints. *Mater. Sci. Eng. Rep.* **2012**, *73*, 85–100. [CrossRef]
22. Ishiguro, Y.; Tsukada, Y.; Koyama, T. Phase-field Simulation of Spinodal Decomposition and Its Effect on Stress Induced Martensitic Transformation in Ti-Nb-O Alloys. *Comp. Mater. Sci.* **2018**, *151*, 222–230. [CrossRef]
23. Santoki, J.; Mukherjee, A.; Schneider, D.; Selzer, M.; Nestler, B. Phase-field Study of Electromigration-induced Shape Evolution of A Transgranular Finger-like Slit. *J. Electron. Mater.* **2019**, *48*, 182–193. [CrossRef]
24. Dieter, G. *Mechanical Metallurgy*, 3rd ed.; McGraw-Hill: New York, NY, USA, 1986; pp. 212–219.

25. Livak, R.J.; Thomas, G. Spinodally Decomposed Cu-Ni-Fe Alloys of Asymmetrical Compositions. *Acta. Metall.* **1971**, *19*, 497–505. [CrossRef]
26. Sigala-García, D.A.; López-Hirata, V.M.; Saucedo-Muñoz, M.L.; Dorantes-Rosales, H.J.; Villegas-Cárdenas, J.D. Phase-field Simulation of Spinodal Decomposition in Mn-Cu Alloys. *Metals* **2022**, *12*, 1220. [CrossRef]
27. Liu, P.L.; Shang, J.K. Interfacial Embrittlement by Bismuth Segregation in Copper/Tin-Bismuth Pb-free Solder Inter connect. *J. Mater. Res.* **2001**, *16*, 1651–1659. [CrossRef]